Bat and pig IFN-induced transmembrane protein 3 restrict cell entry by influenza virus and lyssaviruses

Camilla T. O. Benfield,[1] Sarah E. Smith,[2] Edward Wright,[3] Rachael S. Wash,[2] Francesca Ferrara,[4] Nigel J. Temperton[4] and Paul Kellam[2,5]

Correspondence
Camilla T. O. Benfield
cbenfield@rvc.ac.uk

[1]Department of Pathology and Pathogen Biology, The Royal Veterinary College, Hatfield, UK

[2]Wellcome Trust Sanger Institute, Wellcome Trust Genome Campus, Hinxton, Cambridge, UK

[3]Viral Pseudotype Unit (Fitzrovia), Faculty of Science and Technology, University of Westminster, London, UK

[4]Viral Pseudotype Unit (Medway), School of Pharmacy, University of Kent, Chatham Maritime, Kent, UK

[5]MRC/UCL Centre for Medical Molecular Virology, Division of Infection and Immunity, University College London, London, UK

IFN-induced transmembrane protein 3 (IFITM3) is a restriction factor that blocks cytosolic entry of numerous viruses that utilize acidic endosomal entry pathways. In humans and mice, IFITM3 limits influenza-induced morbidity and mortality. Although many IFITM3-sensitive viruses are zoonotic, whether IFITMs function as antiviral restriction factors in mammalian species other than humans and mice is unknown. Here, IFITM3 orthologues in the microbat (*Myotis myotis*) and pig (*Sus scrofa domesticus*) were identified using rapid amplification of cDNA ends. Amino acid residues known to be important for IFITM3 function were conserved in the pig and microbat orthologues. Ectopically expressed pig and microbat IFITM3 co-localized with transferrin (early endosomes) and CD63 (late endosomes/multivesicular bodies). Pig and microbat IFITM3 restricted cell entry mediated by multiple influenza haemagglutinin subtypes and lyssavirus glycoproteins. Expression of pig or microbat IFITM3 in A549 cells reduced influenza virus yields and nucleoprotein expression. Conversely, small interfering RNA knockdown of IFITM3 in pig NPTr cells and primary microbat cells enhanced virus replication, demonstrating that these genes are functional in their species of origin at endogenous levels. In summary, we showed that IFITMs function as potent broad-spectrum antiviral effectors in two mammals – pigs and bats – identified as major reservoirs for emerging viruses.

INTRODUCTION

Restriction factors are germline-encoded proteins that function in a cell-autonomous manner to suppress virus replication. The IFN-induced transmembrane (IFITM) proteins are a family of small IFN-stimulated proteins that affect diverse cellular processes (reviewed by Siegrist *et al.*, 2011) and were recently identified as antiviral restriction factors that inhibit the cell entry of multiple pathogenic viruses (Brass *et al.*, 2009).

To date, IFITMs have been reported to restrict the enveloped viruses influenza A, West Nile virus and

dengue virus (family *Flaviviridae*), severe acute respiratory syndrome coronavirus, Ebola virus and Marburg virus (family *Filoviridae*), vesicular stomatitis virus (VSV) and lyssaviruses (family *Rhabdoviridae*), human immunodeficiency virus type 1 and several species of the family *Bunyaviridae*, as well as a non-enveloped orthoreovirus (family *Reoviridae*) (Anafu *et al.*, 2013; Brass *et al.*, 2009; Huang *et al.*, 2011; Jia *et al.*, 2012; Lu *et al.*, 2011; Mudhasani *et al.*, 2013; Smith *et al.*, 2013; Weidner *et al.*, 2010). The common feature of IFITM-sensitive viruses appears to be their dependence on acidic endosomal entry pathways, either for proteolytic cleavage, or for pH- or protease-dependent activation of viral entry proteins into their fusogenic form. Accordingly, pseudotyped retroviruses expressing heterologous surface envelope proteins

Four supplementary figures are available with the online Supplementary Material.

recapitulate the IFITM sensitivity of the authentic virus from which the envelope protein derives, and have been widely used to study IFITM biology (Brass *et al.*, 2009; Feeley *et al.*, 2011; Huang *et al.*, 2011). IFITMs localize to membranes of late endosomes and lysosomes and prevent the release of viral particles from these compartments into the cytosol (Feeley *et al.*, 2011).

The human *IFITM* gene family comprises *IFITM1*, *-2*, *-3* and *-5*, all of which possess antiviral activity and cluster together on chromosome 11, as well as *IFITM10* whose function remains unknown. Mice possess orthologues of all the human *IFITM* genes and two additional genes, *Ifitm6* and *-7*. IFITM1, -2 and -3 are expressed in a wide range of tissues (Bailey *et al.*, 2012; Everitt *et al.*, 2013; Siegrist *et al.*, 2011) whereas IFITM5 expression is limited to osteoblasts (Moffatt *et al.*, 2008). Of all the IFITMs, IFITM3 is the most potent anti-influenza effector *in vitro* (Huang *et al.*, 2011). Ifitm3 has a critical role in limiting influenza-induced morbidity and mortality in mice (Everitt *et al.*, 2012). As the phenotype of influenza-infected *Ifitm3*$^{-/-}$ mice is indistinguishable from that of mice deleted for the entire locus (comprising *Ifitm1*, *-2*, *-3*, *-5* and *-6*), Ifitm3 apparently dominates influenza resistance *in vivo* (Bailey *et al.*, 2012). Moreover, the importance of IFITM3 was highlighted by reports showing that an *IFITM3* allele (rs12252-C) is associated with enhanced disease severity caused by pandemic influenza virus H1N1/09 (Everitt *et al.*, 2012; Zhang *et al.*, 2013b) and highly pathogenic influenza virus H7N9 (Wang *et al.*, 2014) and is more frequent in Chinese than in Caucasian populations.

IFITM proteins comprise a relatively long hydrophilic N-terminal region, two hydrophobic intramembrane domains (IM1 and IM2) separated by a conserved intracellular loop (CIL), and a comparatively short hydrophilic C-terminal region. IM1 and CIL together constitute the CD225 domain, a functionally poorly defined domain shared by >300 members of the CD225/pfam04505 protein super-family. Several alternative topologies have been proposed for the IFITMs (Chen *et al.*, 1984; Li *et al.*, 2013; Takahashi *et al.*, 1990; Yount *et al.*, 2012), but the most recent study suggests that murine Ifitm3 is a type II transmembrane protein, comprising an intracellular N terminus, an extracellular C terminus and a membrane-spanning 'IM2' domain (Bailey *et al.*, 2013). IFITM function is regulated by several post-translational modifications. *S*-Palmitoylation of IFITM3 on three membrane-proximal cysteine residues enhances membrane affinity and antiviral activity against influenza (Yount *et al.*, 2010, 2012). Conversely, lysine-linked ubiquitination decreases the co-localization of IFITM3 with endolysosomes and its antiviral potency (Yount *et al.*, 2012). The Y20 residue, which can be phosphorylated by the tyrosine kinase Fyn, is critical for targeting IFITM3 to endolysosomes and for restriction of endosome-dependent viruses (Jia *et al.*, 2012; John *et al.*, 2013).

Current evidence indicates that IFITMs block viral entry to the cytosol by preventing fusion between viral and host-cell membranes. IFITMs multimerize via their IM1 regions (John *et al.*, 2013) and increase membrane rigidity (Li *et al.*, 2013). This suggests a model in which IFITMs either physically resist the deformation of the membrane by the viral fusion machinery or hinder the lateral mobility of viral or cellular proteins within the membrane and thereby block successful pore formation (John *et al.*, 2013; Li *et al.*, 2013; Perreira *et al.*, 2013). Amini-Bavil-Olyaee *et al.* (2013) recently reported that IFITM3 interacts with a protein involved with cholesterol homeostasis, vesicle-membrane-protein-associated protein A (VAPA), and thereby causes cholesterol accumulation in multivesicular bodies and late endosomes, which inhibits the fusion between virion and endosomal membranes. However, a unifying mechanism to explain antiviral restriction by IFITM proteins remains elusive (Perreira *et al.*, 2013; Smith *et al.*, 2014). Indeed, recent reports showing that IFITM3 can be co-opted to promote cell entry of human coronavirus OC43 (Zhao *et al.*, 2014) and human papillomavirus (Warren *et al.*, 2014) suggest virus-specific IFITM interactions.

Although the *IFITM* gene family is evolutionarily conserved in vertebrates (Hickford *et al.*, 2012; Zhang *et al.*, 2012), it is unclear whether antiviral activity is also conserved among vertebrate IFITMs. Here, we focused on the bat and pig, as these hosts are particularly relevant to the ecology of several IFITM-sensitive zoonotic viruses.

RESULTS

Sequence analysis of IFITM3 orthologues cloned from microbat and pig cells

In vertebrates, the *IFITM1*, *-2*, *-3* and *-5* genes cluster together in an *IFITM* locus flanked by the *B4GALNT4* and *ATHL1* genes. It was not possible to assign pig and bat IFITM3 orthologues based on conserved synteny due to the lack of a *B4GALNT4* orthologue in pigs, gaps in the genome assemblies and the low sequencing coverage of the bat genomes (2.6× for *Pteropus vampyrus* and 1.7× for *Myotis lucifugus* at the time of analysis). Therefore, to identify *IFITM* genes, rapid amplification of cDNA ends (RACE) was performed on a newborn pig tracheal cell line (NPTr) and primary lung fibroblasts from the greater mouse-eared bat, *Myotis myotis*, a European species of microbat (Vespertilionidae). *M. myotis* was selected as it is a known reservoir host for several highly pathogenic viruses (Amengual *et al.*, 2007; Drexler *et al.*, 2011, 2012) and genomes are available for other species from the same genus (Seim *et al.*, 2013; Zhang *et al.*, 2013a).

RACE using primers designed to the conserved central regions of compiled *IFITM*-like sequences yielded several *IFITM* gene variants, of which the designated IFITM3-like sequences were the most abundant. For the pig, the IFITM3-like sequence was the only IFITM variant identified that had an N-terminal extension typical of

IFITM2/3 proteins (compare human IFITM1-3 in Fig. 1b). For the microbat, the sequence we assigned as IFITM3 was the most frequent of several long IFITM variants (68 % of sequenced clones) and the only one encoding a double phenylalanine motif (F8/F9) conserved in the human and pig IFITM3 orthologues but absent from human IFITM2 (Fig. 1b).

Full-length *IFITM3* cDNA sequences were obtained by reverse transcription-PCR, and introns were identified by PCR using genomic DNA, thereby confirming that these were not intronless expressed pseudogenes. The transcript structure for pig and microbat IFITM3 was the same as for other experimentally verified IFITM3 orthologues, comprising two exons, a single intron of similar size to other *IFITM3* genes and a conserved exon–exon junction site (Fig. 1a). BLAST searches revealed that the *IFITM3* sequence from NPTr cells was identical to the *Sus scrofa IFITM3* reference sequence (GenBank accession no. NM_001201382.1), and the closest match for the cloned microbat IFITM3 was a 'predicted *IFITM3*-like' gene from *M. lucifugus* (GenBank accession no. XP_006108229.1, 95 % amino acid identity).

Multiple sequence alignments showed that amino acid residues that are functionally important in murine and human IFITM3 were conserved in the cloned pig and microbat orthologues (Fig. 1b). These included: (i) three cysteine residues that are *S*-palmitoylated (Yount *et al.*, 2010); (ii) several lysine residues modified by ubiquitination (Yount *et al.*, 2012) (including K88, which can be monomethylated; Shan *et al.*, 2013); (iii) the Y20 residue critical for endosomal targeting (Jia *et al.*, 2012; John *et al.*, 2013); (iv) two phenylalanine residues (F75 and F78), which mediate oligomerization (John *et al.*, 2013); and (v) R85, R87 and Y99 shown to influence antiviral restriction (John *et al.*, 2013) (Fig. 1b, shaded residues). The microbat and pig IFITM3 proteins were most divergent from human IFITM3 at their N and C termini, and were most conserved in the central CD225 domain, a pattern shared with other orthologues (chicken and mouse Ifitm3) and paralogues (human IFITM2 and IFITM1) (Fig. 1b).

Microbat and pig IFITM3 localize to transferrin- and CD63-positive endosomes

To analyse the IFITM3 proteins, A549 cells (which express low levels of endogenous IFITM3; Brass *et al.*, 2009) were stably transduced to express C-terminally haemagglutinin (HA)-tagged IFITM3 from pig, microbat or human. Prior work has shown that C-terminal epitope tags do not affect the function or expression levels of IFITM3, and indicate that tagged constructs adopt the same topology as the WT protein (Bailey *et al.*, 2013).

Similar to human IFITM3, both pig and microbat IFITM3 had a punctate intracellular distribution following cell fixation and permeabilization (Fig. 2) and co-localized with endocytosed transferrin (early endosomes) and with CD63, a marker for late endosomes/multivesicular bodies (MVBs),

but not with the lysosomal marker LAMP1 (Fig. 2). There was an enlargement of CD63-positive structures in cells expressing microbat or human IFITM3 in comparison with the smaller CD63-positive vesicles seen in pig IFITM3-expressing or untransduced A549 cells (Fig. 2b). Enlargement of CD63-containing compartments was most marked in cells containing larger foci of IFITM3–HA staining. Microbat IFITM3–HA sometimes co-localized with CD63 in 'hollow' ring-like structures (arrows in Fig. 2b).

Endocytic uptake of microbat and pig IFITM3 from the plasma membrane

To investigate the trafficking of pig and microbat IFITM3 proteins, live cells were incubated with FITC-conjugated anti-HA antibody and Alexa Fluor 546-conjugated transferrin prior to fixation. When labelling was performed on ice, endocytosis was prevented, as indicated by the weak stippled transferrin signal, probably corresponding to clathrin-coated pits pre-internalization (Fig. 3a). Under these conditions, IFITM3 from the three species was detected on the plasma membrane, clearly highlighting filopodia and membrane ruffles, whilst no vesicular staining was observed. In contrast, when labelling was performed at 37 °C to allow endocytosis, anti-HA staining showed that pig, microbat and human IFITM3 formed discrete puncta, which, as observed previously, overlapped or were closely associated with transferrin-positive endosomes (Fig. 3b). For all IFITM3 proteins, internalization of the anti-HA antibody by live cells identified larger, brighter puncta that were more widely distributed within the cytosol compared with the HA staining seen previously following fixation and permeabilization (indicating that permeabilization may cause some extraction of the membrane-associated IFITM3). In conclusion, pig and microbat IFITM3 share the following with their human counterpart: (i) plasma membrane trafficking; (ii) extracellular exposure of their C termini (allowing detection of the C-terminal HA tag in intact cells); and (iii) endocytic uptake from the plasma membrane into the endosomal pathway.

Microbat and pig IFITM3 restrict cell entry mediated by influenza HA

To determine whether pig and microbat IFITM3 restrict influenza A virus entry, lentiviruses expressing the HA proteins from diverse influenza subtypes were used to infect A549 cells that were untransduced or had been transduced to express either human IFITM3, pig IFITM3 (Fig. 4a) or microbat IFITM3 (Fig. 4b). Three independently cloned cell lines of the pig and microbat IFITM3 proteins markedly inhibited the infectivity of all influenza HA subtypes tested, including both group 1 and group 2 HAs and highly pathogenic avian H5 and H7 (Fig. 4). Pig or microbat IFITM3 did not restrict viruses pseudotyped with the entry proteins of the gammaretroviruses amphotrophic murine leukemia virus or Gibbon ape leukemia

(a)

Exon 1

```
CHICKEN_IFITM3   ---------------ATGGAGCGGGTACGCGCTTCGGGTCCGGGAGTCCCACCG---TAT 42
MOUSE_IFITM3     ATGAACCACACTTCTCAAGCCTTCATCACCGCTGCCAGTGGAGGACAGCCCCCAAACTAC 60
MICROBAT_IFITM3  ATGAACCCCAACTCCCAGCCCTTCTTCTCTGGCGCCCGCGCCGGAGTGTCCCCATCCTAT 60
PIG_IFITM3       ATGAACTGCGCTTCCCAGCCCTTCTTCACTGGTGCCCATGGAGGA---CCCCCAACATAT 57
HUMAN_IFITM3     ATGAATCACACTGTCCAAACCTTCTTCTCTCCTGTCAACAGTGGCCAGCCCCCCAACTAT 60
                                *                   **      *  **      **

CHICKEN_IFITM3   GAACCCCTGATGGACGGGATGGAC------ATGGAGGGGAAG----------------- 78
MOUSE_IFITM3     GAAAGAATCAAGGAAGAATATGAGGTGGCTGAGATGGGGGCACCGCACGGATCGGCTTCT 120
MICROBAT_IFITM3  GAGGTGCTCAAGGAGGAACACGAGGTGTCTGTGCTGGGGGGTCCCCAGAGCTCGATGGCA 120
PIG_IFITM3       GAGATGCTCAAGGAGGAGCACGAGGTGGCCGTGCTGGGGGGCTCCCCAGACCTCAGCCCC 117
HUMAN_IFITM3     GAGATGCTCAAGGAGGAGCACGAGGTGGCTGTGCTGGGGGGCGCCCCACAACCCTGCTCCC 120
                 **     *  *  *** *       **            *  ****

CHICKEN_IFITM3   ACCCGCAGCACGGTGGTGACGGTG------GAGACGCCCCTGGTGCCTCCTCCCCGCGAC 132
MOUSE_IFITM3     GTCAGAACTACTGTGATCAACATGCCCAGAGAGGTGTCGGTG------------CCTGAC 168
MICROBAT_IFITM3  GCGAGGACGACGGTGGTCAACATCCAGACTGACACAGTGGTG------------CCCGAC 168
PIG_IFITM3       GTGGCCACCACGGTGATCAACATCCGAAGCGAGACCTCCGTG------------CCCGAC 165
HUMAN_IFITM3     CCGACGTCCACCGTGATCCACATCCGCAGCGAGACCTCCGTG------------CCCGAC 168
                        **  ***  *     *       **        **           *  ***

CHICKEN_IFITM3   CACCTGGCCTGGTCGCTGTGCACCACGCTGTACGCCAACGTCTGCTGCCTCGGCTTCCTG 192
MOUSE_IFITM3     CATGTGGTCTGGTCCCTGTTCAATACACTCTTCATGAACTTCTGCTGCCTGGGCTTCATA 228
MICROBAT_IFITM3  CACATCGTCTGGTCCCTGTTCAACACCCTCTTCTTCAACCCCTGCTGCCTGGGCTTCGTG 228
PIG_IFITM3       CACGTCGTCTGGTCCCTGTTCAACACCCTCTTCATGAACTGGTGCTGCCTGGGCTTCGTG 225
HUMAN_IFITM3     CATGTCGTCTGGTCCCTGTTCAACACCCTCTTCATGAACCCCTGCTGCCTGGGCTTCATA 228
                 **  *  * ****** **** **  ** ** *  *  ***  ******** ****** *
```

Intron **Exon 2**

```
CHICKEN_IFITM3   GCGCTCGTCTTCTCCGTGAAGgttggggaat….gtctccccagTCCAGGGATCGCAAAGT 230
MOUSE_IFITM3     GCCTATGCCTACTCCGTGAAGgtgagtgtgc….tctgctccagTCTAGGGATCGGAAGAT 266
MICROBAT_IFITM3  GCGTTCGCCTACTCCGTGAAGgtgggtgcgc….tctcccccagTCTAGGGACCGGAAGAT 266
PIG_IFITM3       GCTTTCGCCTACTCCGTGAAGgtgggtgggc….tctcctccagGCGAGGGACCGGAAGAT 263
HUMAN_IFITM3     GCATTCGCCTACTCCGTGAAGgtgcgtatgg….tctcccccagTCTAGGGACAGGAAGAT 266
                 **     *  ** ********          *  *   * *****   * ** *

CHICKEN_IFITM3   CCTGGGTGACTACAGCGGGGCGCTCAGCTATGGCTCCACTGCGAAGTACCTGAACATCAC 290
MOUSE_IFITM3     GGTGGGTGATGTGACTGGAGCCCAGGCCTACGCCTCCACTGCTAAGTGCCTGAACATCAG 326
MICROBAT_IFITM3  GGTGGGAGACGTGATTGGGGCCCAGAGCTATGCGTCCACCGCCAAGTGCCTGAACATCTG 326
PIG_IFITM3       GGTGGGAGACATCATTGGGGCCCAGAGCTATGCCTCCACCGCCAAGTGCCTGAACATCTG 323
HUMAN_IFITM3     GGTTGGCGACGTGACCGGGGCCCAGGCCTATGCCTCCACCGCCAAGTGCCTGAACATCTG 326
                  * *  **   *  ** ** *   *** * *  ***** ** **** **********

CHICKEN_IFITM3   GGCCCATCTGATCAACGTCTTCCTCATCATCCTCATCATCGCCCTGGTTGCCAGTGGCAC 350
MOUSE_IFITM3     CACCTTGGTCCTCAGCATCCTGATGGTTGTTATCACCATTGTTAGTGTC----------- 375
MICROBAT_IFITM3  GGCCGTGGTCTTGGGCCTCCTTGTCATAGTTGCGGTCATCATCGCGGTC----------- 375
PIG_IFITM3       GGCTCTGGTCCTGGGCCTCCTTCTGATCATTGCGTTCATCATCGTTTGCACCACTGGCTC 383
HUMAN_IFITM3     GGCCCTGATTCTGGGCATCCTCATGACCATTCTGCTCATCGTCATCCCA----------- 375
                  *        *   *    * ** *  *       *     ***

CHICKEN_IFITM3   CATCATGGTGGCCAACATCTTCAACCACCAGCAGCAACACCCCGAATTCATTGGACCCAC 410
MOUSE_IFITM3     -ATCATCATTGTTCTTAACGCTCAAAACCTTCACACTTAA------------------- 414
MICROBAT_IFITM3  -GTCGTATTTTACACCTCTGCACTGAAT------CGCGGCTACGTGGGTTCCTATCACCT 428
PIG_IFITM3       CCTGGTAATTTTCCAAGCAGTTCTGCAGCTCATAAAGGATTACAGAGGCTACTAG----- 438
HUMAN_IFITM3     -GTGCTGATCTTCCAGGCCTATGGATAG------------------------------- 402
                  *   *  *                          *

CHICKEN_IFITM3   TTAG--------- 414
MOUSE_IFITM3     -------------
MICROBAT_IFITM3  GCCCCAAGACTGA 441
PIG_IFITM3       -------------
HUMAN_IFITM3     -------------
```

(b)

```
HUMAN_IFITM1      --------------------MHKEEHEVAVLGPPPSTILPRSTVINIHSETSV----PDHV 37
HUMAN_IFITM2      MNHIVQT-FSPVNSGQPPNYEMLKEEQEVAMLGVPHNPAPPMSTVIHIRSETSV----PDHV 57
CHICKEN_IFITM3    -----MERVRASGPGVPP-YEPLMDGMD--MEGK------TRSTVVTV--ETPLVPPPRDHL 46
CHIMPANZEE_IFITM3 MNHTVQTFFSPVNSGQPPNYEMLKEEYEVAVLGAPHNPAPPMSTVIHIRSETSV----PDHV 58
MOUSE_IFITM3      MNHTSQAFITAASSGGQPNYEMLKEEYEVAEMGAPHGSASVRTTVINMPREVSV----PDHV 58
MICROBAT_IFITM3   MNPNSQPFFSGARAGVSPSYEVLKEEHEVSVLGGPQSSMAARTTVVNIQTDTVV----PDHI 58
PIG_IFITM3        MNCASQPFFTGAHGG-PPTYEMLKEEHEVAVLGAPQTSAPVATTVINIRSETSV----PDHV 57
HUMAN_IFITM3      MNHTVQTFFSPVNSGQPPNYEMLKEEHEVAVLGAPHNPAPPTSTVIHIRSETSV----PDHV 58
                           :   :     *       :**: : :    **:
```

N terminus

```
HUMAN_IFITM1      VWSLFNTLFLNWCCLGFIAFAYSVKSRDRKMVGDVTGAQAYASTAKCLNIWALILGILMT 97
HUMAN_IFITM2      VWSLFNTLFMNTCCLGFIAFAYSVKSRDRKMVGDVTGAQAYASTAKCLNIWALILGIFMT 117
CHICKEN_IFITM3    AWSLCTTLYANVCCLGFLALVFSVKSRDRKVLGDYSGALSYGSTAKYLNITAHLINVFLI 106
CHIMPANZEE_IFITM3 VWSLFNTLFMNPCCLGFIAFAYSVKSRDRKMVGDVTGAQAYASTAKCLNIWALILGILMT 118
MOUSE_IFITM3      VWSLFNTLFMNFCCLGFIAYAYSVKSRDRKMVGDVTGAQAYASTAKCLNISTLVLSILMV 118
MICROBAT_IFITM3   VWSLFNTLFFNPCCLGFVAFAYSVKSRDRKMVGDIGAQSYASTAKCLNIWAVVLGLLVI 118
PIG_IFITM3        VWSLFNTLFMNWCCLGFVAFAYSVKARDRKMVGDIIGAQSYASTAKCLNIWALVLGLLLI 117
HUMAN_IFITM3      VWSLFNTLFMNPCCLGFIAFAYSVKSRDRKMVGDVTGAQAYASTAKCLNIWALILGILMT 118
                  .*** .**: * *****:* .:***:****::**  ** :*.**** *** : :: :::
```

IMI   CIL   IM2

CD225 domain

```
HUMAN_IFITM1      IGFILLLVFGSVTVYHIMLQIIQEKRGY------ 125
HUMAN_IFITM2      ILLIIIP----VLVVQAQR-------------- 132
CHICKEN_IFITM3    ILIIALVASGTIMVANIFNHQQQHPEFIGPT--- 137
CHIMPANZEE_IFITM3 ILLIVIP----VLIFQAYG-------------- 133
MOUSE_IFITM3      VITIVSV----IIIVLNAQNLHT---------- 137
MICROBAT_IFITM3   VAVIIAV----VVFYTSALN--RGYVGSYHLPQD 146
PIG_IFITM3        IAFIIVCTTGSLVIFQAVLQLIKDYRGY------ 145
HUMAN_IFITM3      ILLIVIP----VLIFQAYG-------------- 133
                  :   *       : .
```

C terminus

Fig. 1. Multiple sequence alignments with microbat and pig IFITM3. (a) Pig and microbat IFITM3 nucleotide sequences were aligned with experimentally verified IFITM3 orthologues. The intron–exon boundary is shown (exon1: black; exon 2: blue) and intronic sequences flanking the splice sites are in red lower-case letters. An asterisk indicates identical nucleotides. (b) Pig and microbat IFITM3 amino acid sequences were aligned with other IFITM proteins. Text colour of amino acid residues denotes their physiochemical properties: blue: acidic, red: small and hydrophobic, magenta: basic, green: hydroxyl, sulfhydryl, amine and glycine. An asterisk indicates identical amino acid residues, ':' indicates residues with strongly similar properties and '.' indicates residues with weakly similar properties. The arrow indicates the exon–exon boundary. The protein domains of human IFITM3 are shown (according to John *et al.*, 2013): IM1, CIL and IM2. Highlighted residues are discussed within the text.

virus (Fig. S1, available in the online Supplementary Material), consistent with previous studies on human IFITM3 (Brass *et al.*, 2009; Huang *et al.*, 2011).

Microbat and pig IFITM3 inhibit replication-competent influenza virus

To assess the effect of the IFITM3 orthologues on replication-competent influenza virus, untransduced A549 cells or cells expressing either human, pig or microbat IFITM3 were infected with influenza A/WSN/33 (H1N1) and nucleoprotein (NP) expression was quantified using flow cytometry. Expression of either pig or microbat IFITM3 led to a marked reduction in the proportion of NP-positive cells for all cell clones (Fig. 5a). There was a slight variation in the degree of restriction between the three cell lines expressing pig IFITM3 (Figs 5a and Fig. S2) despite comparable expression of IFITM3–HA seen by Western blotting (Fig. S2).

Stable expression of pig, microbat or human IFITM3 in A549 cells significantly reduced single-cycle growth of influenza A/WSN/33 (Fig. 5c), consistent with reduced NP expression measured in parallel (Fig. 5b). Inhibition of virus yields was more profound following a low m.o.i. infection (>1 $\log_{10}$ for pig IFITM3 and >2 $\log_{10}$ for both microbat and human IFITM3) relative to control green fluorescent protein (GFP)-expressing cells (Fig. 5d). A similar pattern of restriction was also observed when NP expression was analysed after infections with an avian-like swine influenza strain, A/swine/453/06 (H1N1) (Fig. 5b). Levels of the stably expressed proteins were examined by Western blotting against the C-terminal HA epitope tag, and showed that pig IFITM3, human IFITM3 and GFP expression were comparable, whilst microbat IFITM3 was more highly expressed (Figs 5b and S3).

Microbat and pig IFITM3 block cell entry mediated by lyssavirus entry proteins

In light of data that suggest there may be virus-specific antiviral determinants of IFITM (John *et al.*, 2013; Zhao *et al.*, 2014), it was of interest to explore the antiviral spectrum of pig and microbat IFITM3, especially for viruses that naturally infect these species.
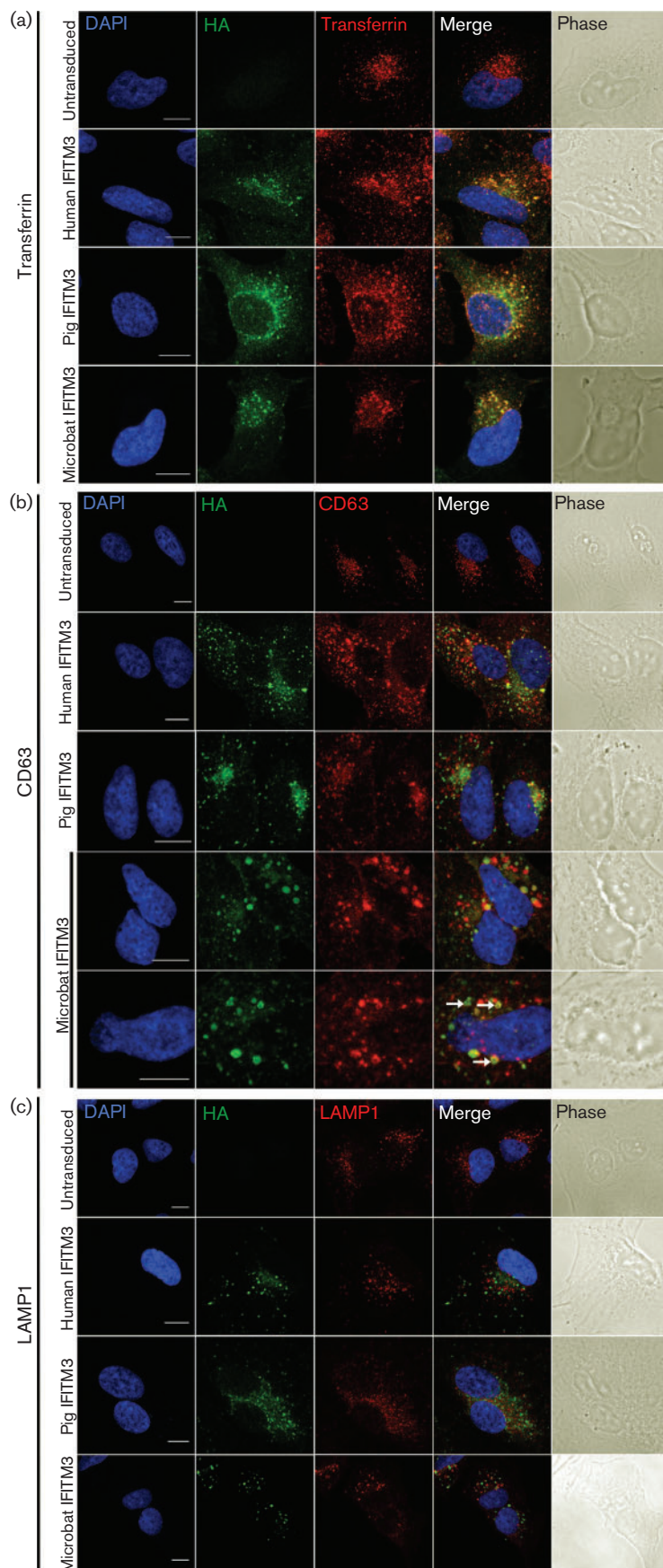
A549 cells stably expressing either pig, microbat or human IFITM3 were infected with pseudotyped lentiviruses that expressed the envelope glycoproteins from isolates representing different lyssavirus phylogroups, namely rabies virus strain Evelyn Rokitniki Abelseth (phylogroup 1), Mokola virus (phylogroup 2), Lagos bat virus (phylogroup 2) and West Caucasian bat virus (phylogroup 3). Expression of IFITM3 from microbat, pig or human reduced infectivity mediated by all four lyssavirus entry proteins, in all cases by approximately 2 $\log_{10}$ relative to the control cells (Fig. 6). Thus, the pig and microbat IFITM3 orthologues inhibit cell entry mediated by multiple lyssavirus glycoproteins (G proteins).

IFITM3 activity in pig and microbat cells

Finally, we addressed the contribution of IFITM3 to antiviral responses in pig and microbat cells. Endogenous IFITM3 expression was measured using TaqMan quantitative reverse-transcription PCR (qRT-PCR) designed to specifically detect IFITM3 mRNA and not other IFITM paralogues identified in these cells by RACE. Baseline levels of IFITM3 mRNA were readily detected in both the porcine NPTr cells [threshold cycle (C_t) value of IFITM3=22.7; C_t value of glyceraldehyde 3-phosphate dehydrogenase (GAPDH)=21.33] and in microbat lung fibroblasts (C_t value of IFITM3 =25.8; C_t value of GAPDH=22.8). IFITM3 induction was assessed in response to the dsRNA analogue poly(I:C), a molecular pattern associated with viral infection, which is recognized by Toll-like receptor 3 and induces type I IFN in porcine (Provost *et al.*, 2012) and bat (Biesold *et al.*, 2011; Omatsu *et al.*, 2008; Zhou *et al.*, 2011) cells. Poly(I:C) addition led to a 3.5-fold increase in pig IFITM3 and a twofold increase in microbat IFITM3 mRNA levels (Fig. 7). The microbat cells were also stimulated via poly(I:C) transfection; as in pteropid bat lung cells (but not primary cells from other tissues) this enhanced IFN-β induction relative to extracellular delivery of poly(I:C) (Zhou *et al.*, 2011). However, transfection of poly(I:C) into microbat cells resulted in a similar degree of IFITM3 induction (2.3-fold) (Fig. 7).

Next, the function of endogenous IFITM3 was assessed using small interfering RNA (siRNA) designed using the RACE sequence data to target IFITM3 and not other putative IFITM paralogues. siRNA targeting IFITM3 or control non-targeting siRNAs were transfected into cells with poly(I:C) induction of IFITM3. IFITM3 mRNA was quantified by qRT-PCR and the biological effect of the knockdown assessed by infection with influenza A/WSN/33 (Fig. 8). Transfection of siRNA against pig IFITM3 led to a 63 % knockdown in IFITM3 mRNA (fold change of

Fig. 2. Subcellular localization of IFITM3 proteins. A549 cells stably expressing HA-tagged IFITM3 proteins from human, pig or microbat (or untransduced cells) were fixed, permeabilized and stained for HA, CD63 (b) or LAMP1 (c). In (a) cells were incubated with Alexa Fluor 546-conjugated transferrin before fixation and staining with FITC-conjugated anti-HA. Nuclei were stained with DAPI and the coverslips examined by confocal microscopy. Images show representative staining patterns, and merged images are also shown. The right-hand column shows phase-contrast images. Bar, 10 μm. Arrows in (b) identify 'ring-like' staining of microbat IFITM3–HA and CD63.
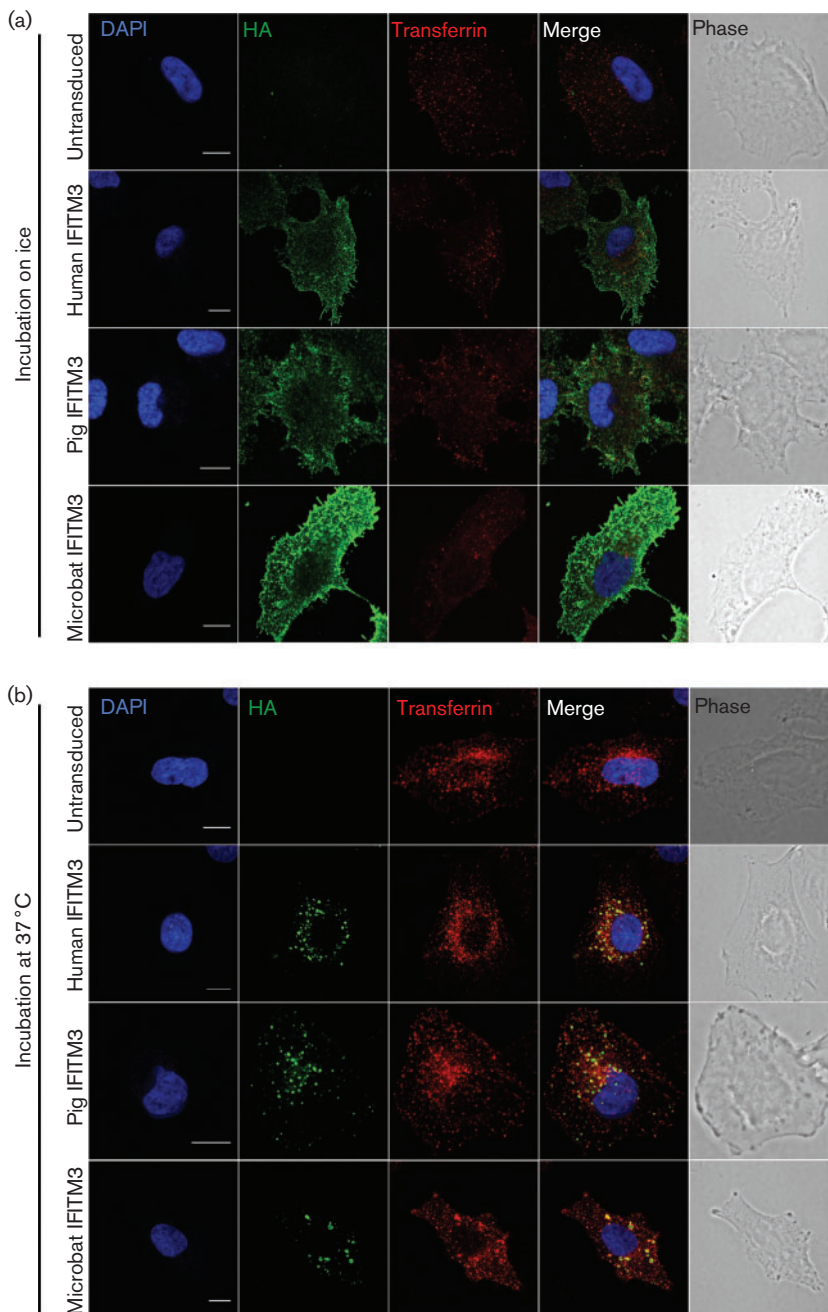
Fig. 3. Endocytic uptake of IFITM3 proteins. Live A549 cells expressing HA-tagged IFITM3 from human, pig or microbat (or untransduced cells) were incubated either on ice (a) or at 37 °C (b) with FITC-conjugated anti-HA and Alexa Fluor 546-conjugated transferrin. After cell fixation, nuclei were stained with DAPI and the coverslips examined by confocal microscopy. The two right-hand columns showed merged images and phase-contrast images. Bar, 10 μm.

1.4 log$_2$) (Fig. 8a), a 3.4-fold increase in virus yield (Fig. 8b) and a twofold increase in the proportion of influenza NP-positive cells (Fig. 8c) relative to control siRNA-transfected cells. In the absence of poly(I:C) stimulation, IFITM3 knockdown in NPTr cells increased influenza NP-positive cells more (3.3-fold) (Fig. 8d), suggesting that additional poly(I:C)-induced genes complement IFITM3-mediated influenza virus restriction. Microbat IFITM3 knockdown in the absence of poly(I:C) stimulation (Fig. 8e–g) reduced IFITM3 mRNA levels by 60 % (fold change of 1.3 log$_2$) (Fig. 8e) and led to a twofold increase in infectious yields (Fig. 8f) and a threefold increase in NP

expression (Fig. 8g), relative to control siRNA transfection. Thus, endogenous IFITM3 in pig tracheal NPTr cells and microbat lung cells restricts influenza virus. Lastly, following siRNA knockdown of baseline IFITM3 in a microbat cell line, overexpression of microbat IFITM3 significantly inhibited influenza NP expression (Fig. S4).

DISCUSSION

Species differences in restriction factors can determine differential viral susceptibility (Duggal & Emerman, 2012; Fadel & Poeschla, 2011; Kirmaier *et al.*, 2010; McNatt *et al.*,
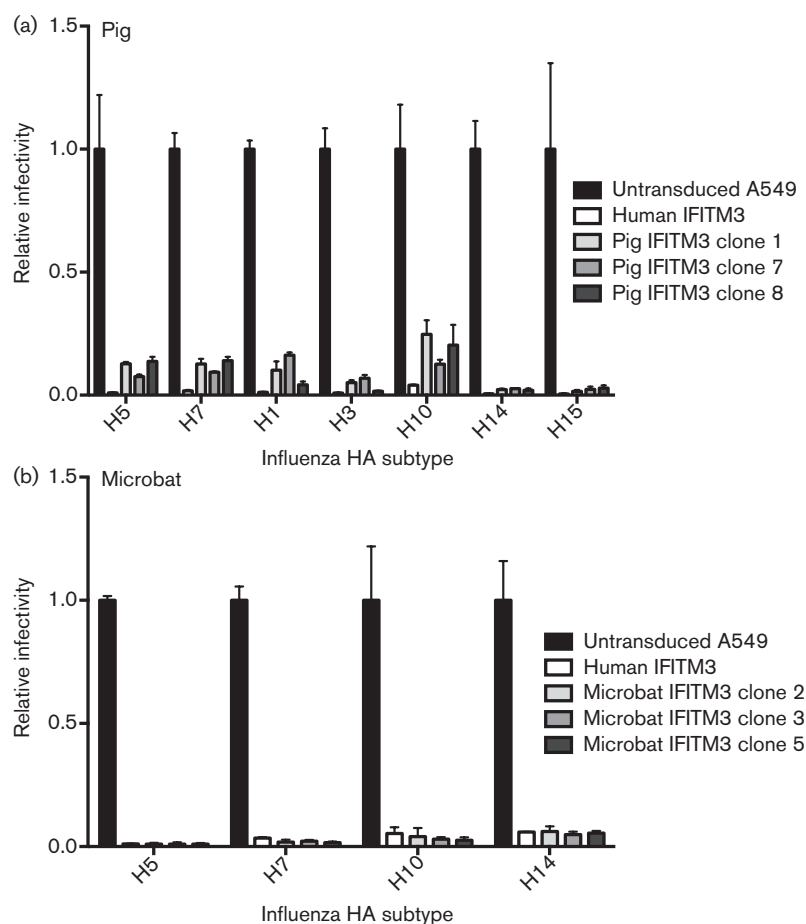
Fig. 4. Microbat and pig IFITM3 inhibit influenza HA-mediated cell entry. A549 cells stably expressing IFITM3 from human, pig (a) or microbat (b) (or untransduced cells) were infected with pseudotyped viruses which express different influenza HA glycoproteins. At 48 h post-infection, luciferase reporter activity was measured and normalized to untransduced cells (relative infectivity of 1 corresponding to 3000–5000 relative light units according to pseudotype used). Results are shown as means $\pm$ SD ($n=3$), and data are representative of three independent experiments.

2009). However, antiviral immunity in reservoir and spill-over hosts remains poorly understood, although important for understanding viral emergence (Bean *et al.*, 2013). Here, we showed that IFITM3 proteins with broad-spectrum antiviral function are conserved in swine and a member of the order Chiroptera, hosts of numerous zoonotic viruses.

The RACE reactions used here captured multiple possible expressed IFITM paralogues by using primers against the conserved CD225 domain. We assigned microbat IFITM3 using several criteria. First, it encoded a double phenyl-alanine motif (F8/F9) found only in other IFITM3 orthologues (whereas the other microbat IFITM variants resembled human IFITM2 in having a single phenylalanine at this position). Secondly, the microbat IFITM3 had an intracellular location and co-localized with endosomal markers. Conserved genome synteny was used previously to help assign *IFITM* genes (Smith *et al.*, 2013; Zhang *et al.*, 2012), but was of limited use in the case of the poorly assembled *IFITM* loci in the pig and microbat genomes. Moreover, the *IFITM* gene family is associated with numerous processed pseudogenes, gene duplications and copy-number variation (Siegrist *et al.*, 2011; Zhang *et al.*, 2012), which significantly complicate the assignment of gene orthology. Although a recent computational study identified eight pig *IFITM* family members with expressed

sequence tag evidence (Miller *et al.*, 2014), it lacked the functional validation presented here.

Functionally important amino acid residues for human or mouse IFITM3 were conserved in pig and microbat IFITM3, indicating that these may be functionally import-ant sites across the orthologues. Amino acid residues are less conserved within IM2 compared with IM1, although IM2 can function as a signal anchor for membrane localization (Bailey *et al.*, 2013) and is also sufficient to mediate the IFITM3–VAPA interaction (Amini-Bavil-Olyaee *et al.*, 2013).

We showed here that C-terminally HA-tagged IFITM3 (of human, pig and microbat) was clearly detectable at the plasma membrane after live cell staining. These data support recent evidence for a luminal (i.e. extracellular) exposure of the C terminus (Bailey *et al.*, 2013), and indicate that pig and microbat IFITM3 adopt a similar topology. Other studies have also reported that a proportion of human IFITM3 localizes to the plasma membrane (Amini-Bavil-Olyaee *et al.*, 2013; Bailey *et al.*, 2013; Brass *et al.*, 2009), and it is thought that the [20]YEML[23] motif acts as a lysosomal sorting signal for the internalization of IFITM3 into the endosomal pathway (Jia *et al.*, 2012; John *et al.*, 2013). Pig and microbat IFITM3
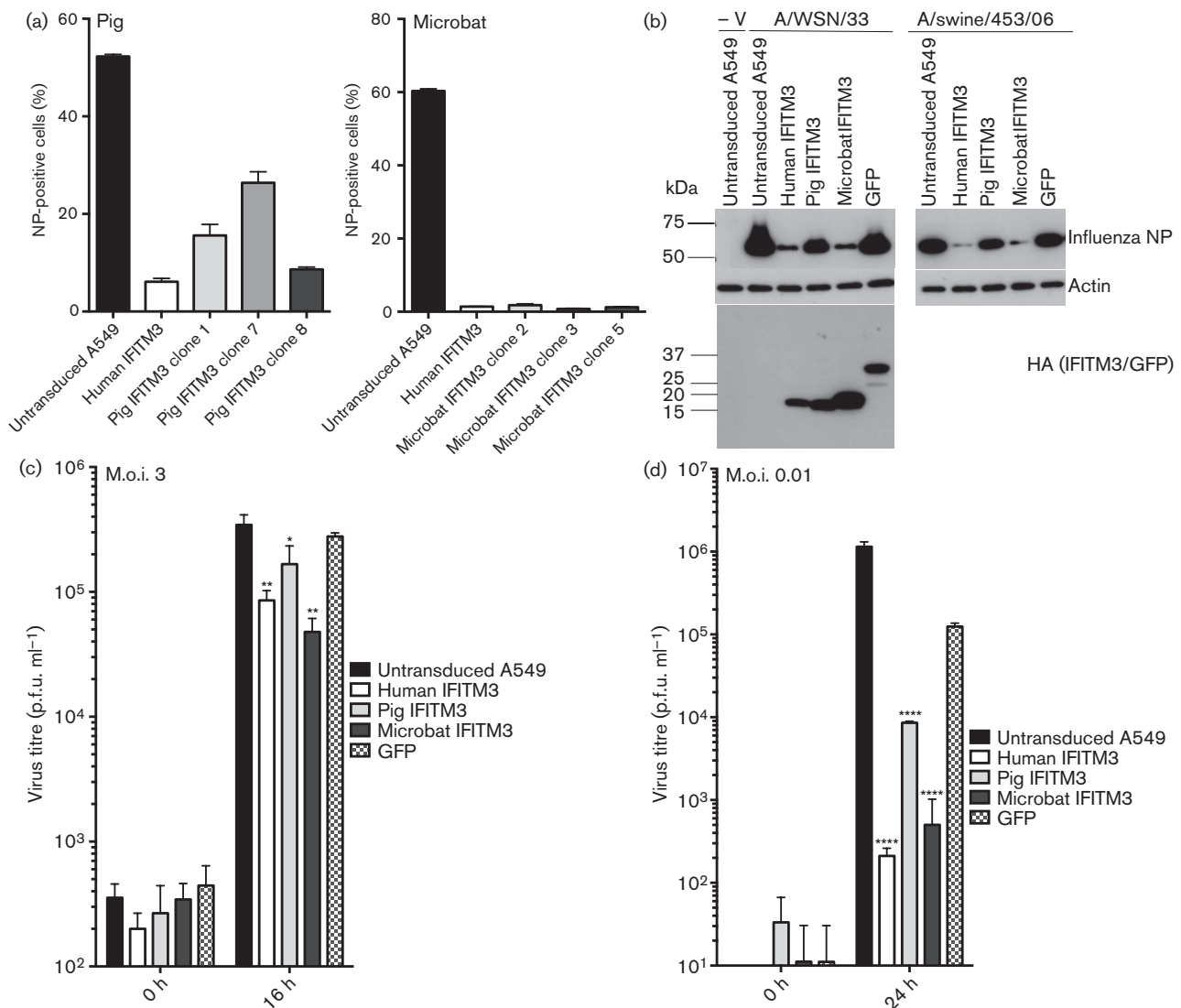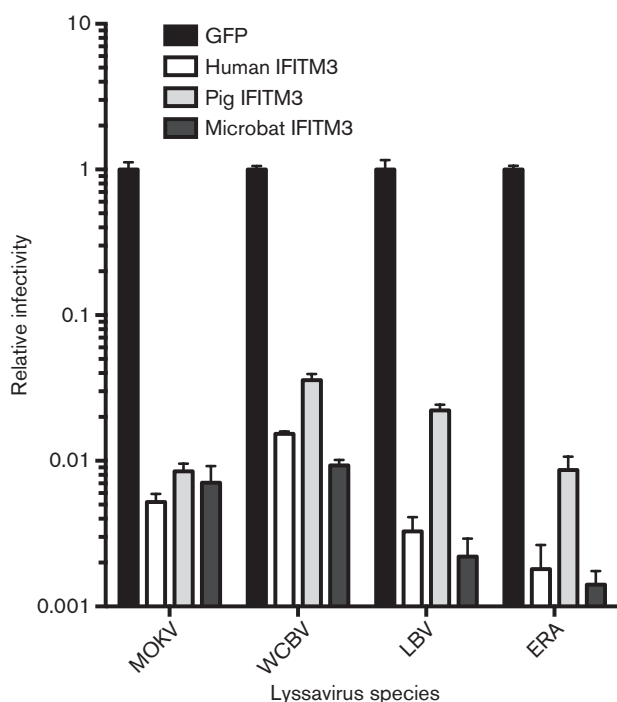
Fig. 5. Microbat and pig IFITM3 inhibit influenza virus replication. A549 cells stably expressing human, pig or microbat IFITM3 were infected with influenza A virus. (a) At 7 h after infection with influenza A/WSN/33, NP expression was analysed by flow cytometry. (b) At 16 h after infection with influenza A/WSN/33 or A/swine/453/06 or mock infection (−V) cells were lysed and Western blotting was performed to detect influenza NP, actin and HA-tagged IFITM3 or green fluorescent protein (GFP). The molecular mass (kDa) of protein size markers is indicated. (c, d) Virus yields following infection with influenza A/WSN/33 at an m.o.i. of 3 (c) or an m.o.i. of 0.01 (d) were measured using plaque assays. Results are shown as means ± SD (n=3). In (b)–(d) pig IFITM3 clone 1 and microbat IFITM3 clone 2 were used. *P<0.05; **P<0.01; ****P<0.0001 relative to GFP-expressing cells (Student's t-test).

contain [20]YEML[23] and [20]YEVL[23], respectively (which conform to the consensus sequence for a tyrosine-based sorting signal YxxΦ, where Φ is a residue with a bulky hydrophobic side chain; Bonifacino & Traub, 2003), and likewise were observed to traffic into endosomes following their cell-surface staining. Pig and microbat IFITM3 co-localized with endocytosed transferrin (early endosomes) and CD63 (late endosomes/MVBs) as seen for human IFITM3 (Figs 2 and 3) (Amini-Bavil-Olyaee et al., 2013; Feeley et al., 2011; Huang et al., 2011; Jia et al., 2012; Lu et al., 2011). Expression of both microbat and human

IFITM3 caused expansion of CD63-positive endosomal compartments, consistent with the documented ability of IFITM3 to induce MVB formation (Amini-Bavil-Olyaee et al., 2013). Furthermore, in some cells, microbat IFITM3 co-stained with CD63 in ring-like structures, a phenomenon reported for human IFITM3 and enhanced by overexpression of its interaction partner, VAPA (Amini-Bavil-Olyaee et al., 2013). In our hands, neither human IFITM3 nor its pig and microbat orthologues co-localized with the lysosomal marker LAMP1, which is consistent with some (Yount et al., 2010) but not other (Feeley et al.,

Fig. 6. Microbat and pig IFITM3 inhibit cell entry mediated by lyssavirus G proteins. A549 cells stably expressing GFP, human IFITM3, pig IFITM3 (clone 1) or microbat IFITM3 (clone 2) were infected with pseudotyped viruses that expressed the envelope glycoprotein from Mokola virus (MOKV), West Caucasian bat virus (WCBV), Lagos bat virus (LBV) or rabies virus strain Evelyn Rokitniki Abelseth (ERA). At 48 h post-infection, luciferase reporter activity was measured and normalized to GFP-expressing cells (relative infectivity of 1 corresponding to 25 000–80 000 relative light units according to pseudotype used). Results are shown as means $\pm$ SD ($n=3$) and data are representative of three independent experiments.

2011; Huang *et al.*, 2011) reports for IFITM3 localization. These discrepancies regarding localization may be due to the multiple post-translational modifications of IFITM3 (Yount *et al.*, 2012) and/or cell type-dependent differences in its topology (Bailey *et al.*, 2013).

We showed that both pig and microbat IFITM3 restricted cell entry mediated by multiple influenza A virus HA (a class I fusion protein) and lyssavirus G (a class III fusion protein) proteins. Restriction at the level of cell entry correlated with significant inhibition of influenza virus yields and NP expression. The microbat, pig and human IFITM3-expressing A549 cells varied in their IFITM3 expression levels, which may underlie variation seen in the degree of restriction. However, anti-influenza restriction by pig IFITM3 was in general lower than that seen for human IFITM3, despite comparable expression levels. We found that pig and human IFITM3 could restrict avian, swine and human influenza A subtypes. Similarly, chicken IFITM3 inhibited viral pseudotypes bearing HAs from both

avian and human strains (Smith *et al.*, 2013). siRNA knockdown of endogenous pig and microbat IFITM3 enhanced influenza replication by a similar degree to that seen following knockdown of human IFITM3 (Huang *et al.*, 2011) or chicken IFITM3 (Smith *et al.*, 2013). IFITM3 was expressed constitutively in pig and bat cells (as reported for other IFITM3 orthologues; Bailey *et al.*, 2012; Everitt *et al.*, 2012, 2013; Friedman *et al.*, 1984; Smith *et al.*, 2013). Baseline levels of IFITM3 in the pig and bat cells were sufficient to limit virus replication and, following siRNA targeting of baseline IFITM3, microbat IFITM3 was also capable of restricting influenza virus when overexpressed in microbat cells. As pig IFITM3 was moderately induced by poly(I:C) and upregulated upon viral challenge *in vivo* (Andersson *et al.*, 2011; Miller *et al.*, 2014), pig IFITM3 is likely to be relevant to host antiviral responses.

Here, we showed that influenza A viruses and lyssaviruses, virus families that share an ancient co-evolutionary history with bats (Badrane & Tordo, 2001; Tong *et al.*, 2013), are restricted by microbat IFITM3. Bats harbour many diverse virus types and are important reservoirs of zoonotic infections (Drexler *et al.*, 2014; Quan *et al.*, 2013; Smith & Wang, 2013; Tong *et al.*, 2013). However, the basis for the intimate association between bats and viruses remains enigmatic, particularly the relative importance of immunological compared with ecological or life history factors (Kupferschmidt, 2013). Although transcriptional induction of chiropteran IFN-stimulated gene orthologues has been reported (Papenfuss *et al.*, 2012; Zhou *et al.*, 2013), there is a striking lack of functional data for any of these genes. We demonstrated that bats do encode functional IFITM3 and therefore are likely to be competent in this aspect of intrinsic antiviral restriction.

METHODS

Cells. A549 cells were maintained in F12 medium, and 293T, NPTr (Ferrari *et al.*, 2003) and FLN-R cells (Friedrich-Loeffler-Institut) were grown in Dulbecco's Modified Eagle's Medium (DMEM) with 10 % FCS. Primary lung cells from the microbat (*M. myotis*) were grown in DMEM containing 10 % FCS, penicillin (100 units ml^{-1}) and streptomycin (100 µg ml^{-1}) and 20 % amnioMAX (Gibco).

RACE and IFITM3 cloning. NPTr and microbat cells were transfected with poly(I:C) (Invivogen) at 33 µg ml^{-1} using Lipofectamine 2000, and 4 h later, total RNA and genomic DNA were isolated (Qiagen AllPrep kit). 5′ and 3′ IFITM cDNA fragments were generated using a SMARTer RACE cDNA amplification kit (Clontech) and the following primers: 5Bat: 5′-GCCCAGAGCTATGCGTCCACCGCCAAGTGCC-3′, and 3Bat: 5′-CGTCTGGTCCCTGTTCAACACCCTCTTC-3′; and 5Pig: 5′-GATGTTCAGGCACTTGGCGGTGGAGGCATAGCTC-3′, and 3Pig: 5′-TGAACTGGTGCTGCCTGGGCTTCGTGG-3′. PCR products were TA cloned and multiple clones were sequenced using Sanger sequencing. Non-coding sequences identified by RACE were used to design primers for PCR amplification of full-length IFITM3 (BatIFITM3ncrF: 5′-GCATCCACACGCCATCTGCTC-3′, and BatIFITM3ncrR: 5′-GAACGCCATTGTGCACATGTGC-3′; and PigIFITM3ncrF: 5′-ACAGCTTCTCCTGGGCACCATG-3′, PigIFITM3ncrR: 5′-GTATGTGCTGCTGTGAAAGGAG-3′). Pig IFITM3 and microbat
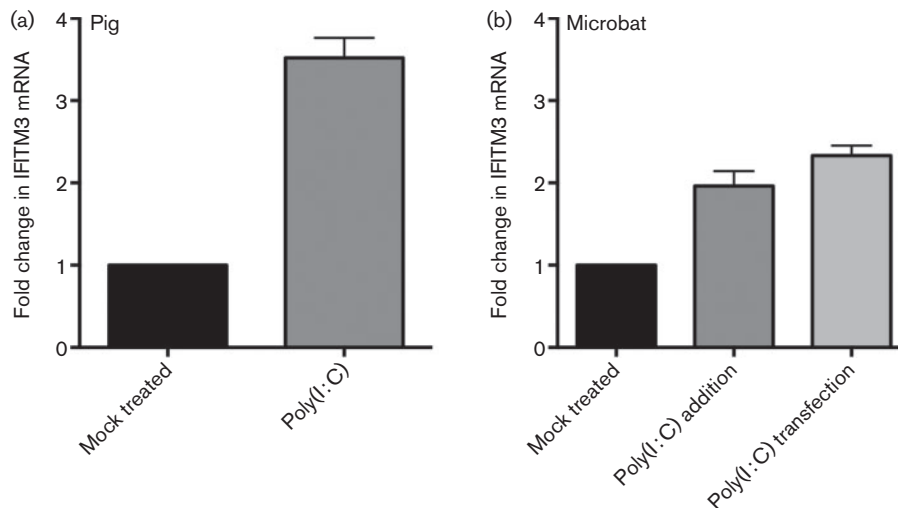
Fig. 7. Microbat and pig IFITM3 are poly(I:C) responsive. Pig NPTr (a) and microbat (b) cells were either mock treated or stimulated by addition of poly(I:C) to the cell medium (50 µg ml^{-1}) or transfection of poly(I:C) (33 µg ml^{-1}) using Lipofectamine 2000 (microbat cells only). After 7 h, qRT-PCR was used to quantify IFITM3 and the reference gene, GAPDH. The fold change in IFITM3 mRNA is expressed relative to mock-treated cells. Results are shown as means $\pm$ SD for biological triplicates assayed in duplicate.

IFITM3 were synthesized as codon-optimized genes for expression in human cells (GeneArt) and cloned into the *Bam*HI and *Not*I sites of the lentivirus vector pSIN-BNHA (derived from pHRSIN-CSGW; Demaison *et al.*, 2002).

Creation of IFITM3-expressing cell lines. Lentiviruses expressing IFITM3 (or GFP as a control) were produced by co-transfecting 293T cells using Fugene HD with the packaging plasmid p8.91 (Zufferey *et al.*, 1997) (1 µg), the VSV-G-expressing plasmid pMDG (1 µg) and the lentivirus vector pSIN-BNHA (1.5 µg) containing either pig IFITM3, microbat IFITM3 or GFP. Supernatants were harvested at 48 and 72 h, filtered (0.45 µm) and used to transduce A549 cells. Transduction efficiency was checked after 48 h by flow cytometric detection of HA. Single-cell clones were generated using limiting dilution and analysed for HA expression. Those with the most similar expression levels were selected for experiments. Human IFITM3-expressing A549 cells were generated using the same method (Smith *et al.*, 2013).

Pseudotyped lentivirus cell entry assay. Lentiviral pseudotypes were produced as described previously (Ferrara *et al.*, 2012; Wright *et al.*, 2008). For the entry assay, A549 cells were seeded in white 96-well plates (10^4 cells per well) 1 day prior to infection with luciferase-expressing pseudotypes expressing influenza HA (GenBank accession nos: H1, AAD17229.1; H5, ABP51969.1; H10, ABI84534.1; H14, BAF43460.1; H7, CAD37074.1; H3, AAA43099.1; H15, AAA96134.1), the G proteins from Mokola virus (MOKV.98/071 RA361; GQ500108), Lagos bat virus (LBV.NIG56-RV1; HM623779), West Caucasian bat virus (AAR03484) or rabies virus Evelyn Rokitniki Abelseth strain (ABN11294) or amphotrophic murine leukemia virus (MLV-A) or gibbon ape leukemia virus (GALV) envelope proteins. The H1 and H3 HAs were human in origin, and the other HA subtypes were avian in origin. Cells were infected in triplicate, and 48 h later, luciferase activity was measured using a Bright-Glo Luciferase Assay System (Promega).

siRNA transfection and qRT-PCR. siRNAs against pig IFITM3 (5′-GCTCATAAAGGATTACAGA-3′) or microbat IFITM3 (5′-

CGAGGACGACGGTGGTCAA-3′) (ON-TARGETplus; Dharmacon) were designed using knowledge of other IFITM paralogues and the Dharmacon siDesign Centre. The ON-TARGETplus non-targeting siRNA pool and an siRNA targeting GFP were used as controls. siRNA was transfected into cells (20 pmol per well of a 12-well plate) using Lipofectamine RNAiMAX. After 48 h, RNA was extracted (RNeasy kit; Qiagen) and a Quantitect multiplex RT-PCR kit (Qiagen) was used to measure *IFITM3* and *GAPDH* simultaneously using TaqMan gene expression assays (Applied Biosystems; primer sequences available on request). MxPro software was used for comparative quantification of *IFITM3* relative to the *GAPDH* reference gene.

Flow cytometry. Cells were infected in triplicate with influenza A/WSN/33 in medium containing 2 % FCS. Cells were trypsinized, fixed using BD Fixation/Permeabilization solution for 20 min and washed twice in BD Perm/Wash buffer before incubation with FITC-conjugated anti-influenza NP IgG (Abcam) for 40 min at 4 °C. After staining, the cells were washed, resuspended in PBS and analysed using a Becton Dickinson FACSCalibur and Cell Quest Pro. For each sample, 10 000 cells (gated by forward and side scatter) were analysed for FITC fluorescence.

Western blotting. After cell lysis using RIPA buffer, proteins were separated by SDS-PAGE (4–12 % TGX gel; Bio-Rad) and transferred to nitrocellulose membrane. After blocking (5 % Marvel, 0.1 % Tween 20 in PBS), the membranes were incubated for 1 h at room temperature with antibodies against influenza NP, β-actin or the HA tag (clone HA.C5; all from Abcam). HRP-conjugated secondary antibodies were used followed by enhanced chemiluminescent detection.

Virus yield assay. Cells were infected in triplicate with influenza A/WSN/33 in medium containing 2 % FCS. After 1 h infection at 37 °C, the cells were washed three times in PBS. At the indicated times post-infection, supernatants were harvested and the virus yields titrated on MDCK cells by plaque assay (Matrosovich *et al.*, 2006).
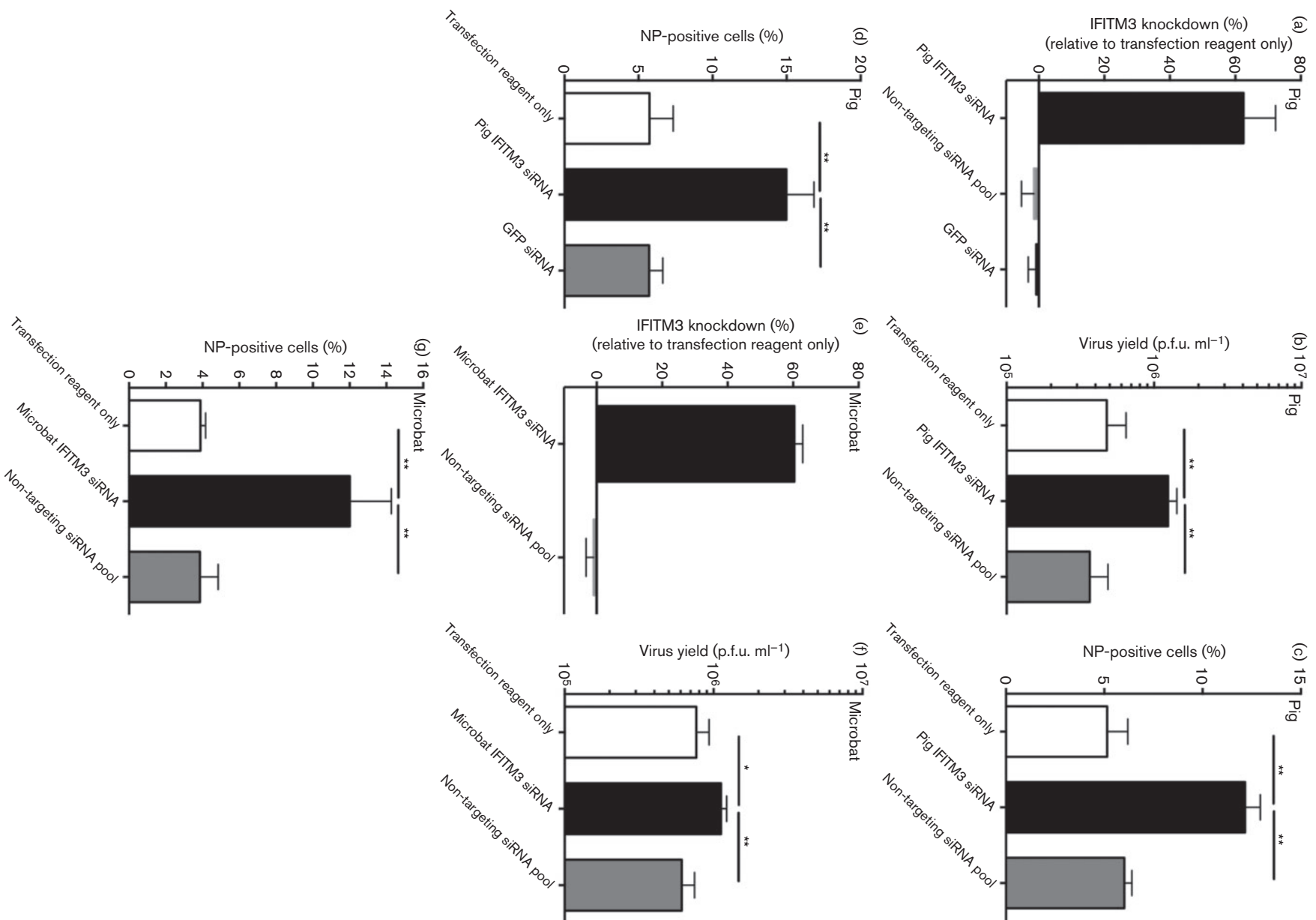
Fig. 8. siRNA knockdown of IFITM3 in pig and microbat cells enhances influenza virus replication. Pig NPTr or microbat cells were transfected with siRNA targeting IFITM3 or control siRNA prior to quantification of IFITM3 by qRT-PCR (a, e) or infection with influenza A/WSN/33. Virus yields were measured by plaque assay (b, f) or NP expression was measured using flow cytometry (c, d, g). NPTr cells were either stimulated with poly(I : C) for 2 h before infection (m.o.i. 0.01) and analysed at 36 h post-infection (b, c) or cells were infected in the absence of poly(I : C). Results are shown as means $\pm$ SD for biological triplicates assayed in duplicate and data are representative of two independent experiments. *$P<0.05$; **$P<0.01$ (Student's t-test).

Immunofluorescence. Cells were fixed with 4 % paraformaldehyde (20 min at room temperature). For transferrin co-localization, cells were pre-incubated with Alexa Fluor 546-conjugated transferrin (5 µg ml^{-1}; Molecular Probes) for 10 min before fixation. Cells were permeabilized using 0.2 % Triton X-100, blocked using antibody buffer (0.1 % Tween 20 and 10 % goat serum in PBS) and stained with FITC-conjugated anti-HA (Bethyl Laboratories), anti-LAMP1 (clone H4A3; Abcam) or anti-CD63 (Santa Cruz Biotechnology) for 1 h at room temperature. Dylight 594-conjugated goat anti-mouse IgG was used to detect the anti-CD63 and anti-LAMP1 antibodies. Live cell staining was performed at 37 °C or on ice, with solutions equilibrated accordingly. Cells were washed twice in serum-free medium before incubation for 30 min with FITC-conjugated anti-HA and Alexa Fluor 546-conjugated transferrin (in serum-free medium). Cells were then washed quickly in PBS and fixed immediately using 4 % paraformaldehyde (20 min). Coverslips were mounted using ProLong Gold reagent with DAPI and examined with a Zeiss LSM 780 confocal microscope.

Sequence analysis. Multiple sequence alignments were performed using Clustal Omega (version 1.2.0), and Seaview (Gouy *et al.*, 2010) was used for manual editing.

ACKNOWLEDGEMENTS

REFERENCES

Amengual, B., Bourhy, H., López-Roig, M. & Serra-Cobo, J. (2007). Temporal dynamics of European bat Lyssavirus type 1 and survival of *Myotis myotis* bats in natural colonies. *PLoS ONE* 2, e566.

Amini-Bavil-Olyaee, S., Choi, Y. J., Lee, J. H., Shi, M., Huang, I. C., Farzan, M. & Jung, J. U. (2013). The antiviral effector IFITM3 disrupts intracellular cholesterol homeostasis to block viral entry. *Cell Host Microbe* 13, 452–464.

Anafu, A. A., Bowen, C. H., Chin, C. R., Brass, A. L. & Holm, G. H. (2013). Interferon-inducible transmembrane protein 3 (IFITM3) restricts reovirus cell entry. *J Biol Chem* 288, 17261–17271.

Andersson, M., Ahlberg, V., Jensen-Waern, M. & Fossum, C. (2011). Intestinal gene expression in pigs experimentally co-infected with PCV2 and PPV. *Vet Immunol Immunopathol* 142, 72–80.

Badrane, H. & Tordo, N. (2001). Host switching in Lyssavirus history from the Chiroptera to the Carnivora orders. *J Virol* 75, 8096–8104.

Bailey, C. C., Huang, I. C., Kam, C. & Farzan, M. (2012). Ifitm3 limits the severity of acute influenza in mice. *PLoS Pathog* 8, e1002909.

Bailey, C. C., Kondur, H. R., Huang, I. C. & Farzan, M. (2013). Interferon-induced transmembrane protein 3 is a type II transmembrane protein. *J Biol Chem* 288, 32184–32193.

Bean, A. G., Baker, M. L., Stewart, C. R., Cowled, C., Deffrasnes, C., Wang, L. F. & Lowenthal, J. W. (2013). Studying immunity to zoonotic diseases in the natural host – keeping it real. *Nat Rev Immunol* 13, 851–861.

Biesold, S. E., Ritz, D., Gloza-Rausch, F., Wollny, R., Drexler, J. F., Corman, V. M., Kalko, E. K., Oppong, S., Drosten, C. & Müller, M. A. (2011). Type I interferon reaction to viral infection in interferon-competent, immortalized cell lines from the African fruit bat *Eidolon helvum*. *PLoS ONE* 6, e28131.

Bonifacino, J. S. & Traub, L. M. (2003). Signals for sorting of transmembrane proteins to endosomes and lysosomes. *Annu Rev Biochem* 72, 395–447.

Brass, A. L., Huang, I. C., Benita, Y., John, S. P., Krishnan, M. N., Feeley, E. M., Ryan, B. J., Weyer, J. L., van der Weyden, L. & other authors (2009). The IFITM proteins mediate cellular resistance to influenza A H1N1 virus, West Nile virus, and dengue virus. *Cell* 139, 1243–1254.

Chen, Y. X., Welte, K., Gebhard, D. H. & Evans, R. L. (1984). Induction of T cell aggregation by antibody to a 16kd human leukocyte surface antigen. *J Immunol* 133, 2496–2501.

Demaison, C., Parsley, K., Brouns, G., Scherr, M., Battmer, K., Kinnon, C., Grez, M. & Thrasher, A. J. (2002). High-level transduction and gene expression in hematopoietic repopulating cells using a human immunodeficiency [correction of imunodeficiency] virus type 1-based lentiviral vector containing an internal spleen focus forming virus promoter. *Hum Gene Ther* 13, 803–813.

Drexler, J. F., Corman, V. M., Wegner, T., Tateno, A. F., Zerbinati, R. M., Gloza-Rausch, F., Seebens, A., Müller, M. A. & Drosten, C. (2011). Amplification of emerging viruses in a bat colony. *Emerg Infect Dis* 17, 449–456.

Drexler, J. F., Corman, V. M., Müller, M. A., Maganga, G. D., Vallo, P., Binger, T., Gloza-Rausch, F., Cottontail, V. M., Rasche, A. & other authors (2012). Bats host major mammalian paramyxoviruses. *Nat Commun* 3, 796.

Drexler, J. F., Corman, V. M. & Drosten, C. (2014). Ecology, evolution and classification of bat coronaviruses in the aftermath of SARS. *Antiviral Res* 101, 45–56.

Duggal, N. K. & Emerman, M. (2012). Evolutionary conflicts between viruses and restriction factors shape immunity. *Nat Rev Immunol* 12, 687–695.

Everitt, A. R., Clare, S., Pertel, T., John, S. P., Wash, R. S., Smith, S. E., Chin, C. R., Feeley, E. M., Sims, J. S. & other authors (2012). IFITM3 restricts the morbidity and mortality associated with influenza. *Nature* 484, 519–523.

Everitt, A. R., Clare, S., McDonald, J. U., Kane, L., Harcourt, K., Ahras, M., Lall, A., Hale, C., Rodgers, A. & other authors (2013). Defining the range of pathogens susceptible to Ifitm3 restriction using a knockout mouse model. *PLoS ONE* 8, e80723.

Fadel, H. J. & Poeschla, E. M. (2011). Retroviral restriction and dependency factors in primates and carnivores. *Vet Immunol Immunopathol* **143**, 179–189.

Feeley, E. M., Sims, J. S., John, S. P., Chin, C. R., Pertel, T., Chen, L. M., Gaiha, G. D., Ryan, B. J., Donis, R. O. & other authors (2011). IFITM3 inhibits influenza A virus infection by preventing cytosolic entry. *PLoS Pathog* **7**, e1002337.

Ferrara, F., Molesti, E., Böttcher-Friebertshäuser, E., Cattoli, G., Corti, D., Scott, S. D. & Temperton, N. J. (2012). The human Transmembrane Protease Serine 2 is necessary for the production of Group 2 influenza A virus pseudotypes. *J Mol Genet Med* **7**, 309–314.

Ferrari, M., Scalvini, A., Losio, M. N., Corradi, A., Soncini, M., Bignotti, E., Milanesi, E., Ajmone-Marsan, P., Barlati, S. & other authors (2003). Establishment and characterization of two new pig cell lines for use in virological diagnostic laboratories. *J Virol Methods* **107**, 205–212.

Friedman, R. L., Manly, S. P., McMahon, M., Kerr, I. M. & Stark, G. R. (1984). Transcriptional and posttranscriptional regulation of interferon-induced gene expression in human cells. *Cell* **38**, 745–755.

Gouy, M., Guindon, S. & Gascuel, O. (2010). SeaView version 4: A multiplatform graphical user interface for sequence alignment and phylogenetic tree building. *Mol Biol Evol* **27**, 221–224.

Hickford, D., Frankenberg, S., Shaw, G. & Renfree, M. B. (2012). Evolution of vertebrate interferon inducible transmembrane proteins. *BMC Genomics* **13**, 155.

Huang, I. C., Bailey, C. C., Weyer, J. L., Radoshitzky, S. R., Becker, M. M., Chiang, J. J., Brass, A. L., Ahmed, A. A., Chi, X. & other authors (2011). Distinct patterns of IFITM-mediated restriction of filoviruses, SARS coronavirus, and influenza A virus. *PLoS Pathog* **7**, e1001258.

Jia, R., Pan, Q., Ding, S., Rong, L., Liu, S. L., Geng, Y., Qiao, W. & Liang, C. (2012). The N-terminal region of IFITM3 modulates its antiviral activity by regulating IFITM3 cellular localization. *J Virol* **86**, 13697–13707.

John, S. P., Chin, C. R., Perreira, J. M., Feeley, E. M., Aker, A. M., Savidis, G., Smith, S. E., Elia, A. E., Everitt, A. R. & other authors (2013). The CD225 domain of IFITM3 is required for both IFITM protein association and inhibition of influenza A virus and dengue virus replication. *J Virol* **87**, 7837–7852.

Kirmaier, A., Wu, F., Newman, R. M., Hall, L. R., Morgan, J. S., O'Connor, S., Marx, P. A., Meythaler, M., Goldstein, S. & other authors (2010). TRIM5 suppresses cross-species transmission of a primate immunodeficiency virus and selects for emergence of resistant variants in the new species. *PLoS Biol* **8**, e1000462.

Kupferschmidt, K. (2013). Emerging infectious diseases. Link to MERS virus underscores bats' puzzling threat. *Science* **341**, 948–949.

Li, K., Markosyan, R. M., Zheng, Y. M., Golfetto, O., Bungart, B., Li, M., Ding, S., He, Y., Liang, C. & other authors (2013). IFITM proteins restrict viral membrane hemifusion. *PLoS Pathog* **9**, e1003124.

Lu, J., Pan, Q., Rong, L., He, W., Liu, S. L. & Liang, C. (2011). The IFITM proteins inhibit HIV-1 infection. *J Virol* **85**, 2126–2137.

Matrosovich, M., Matrosovich, T., Garten, W. & Klenk, H. D. (2006). New low-viscosity overlay medium for viral plaque assays. *Virol J* **3**, 63.

McNatt, M. W., Zang, T., Hatziioannou, T., Bartlett, M., Fofana, I. B., Johnson, W. E., Neil, S. J. & Bieniasz, P. D. (2009). Species-specific activity of HIV-1 Vpu and positive selection of tetherin transmembrane domain variants. *PLoS Pathog* **5**, e1000300.

Miller, L. C., Jiang, Z., Sang, Y., Harhay, G. P. & Lager, K. M. (2014). Evolutionary characterization of pig interferon-inducible transmembrane gene family and member expression dynamics in tracheobronchial lymph nodes of pigs infected with swine respiratory disease viruses. *Vet Immunol Immunopathol* **159**, 180–191.

Moffatt, P., Gaumond, M. H., Salois, P., Sellin, K., Bessette, M. C., Godin, E., de Oliveira, P. T., Atkins, G. J., Nanci, A. & Thomas, G. (2008). Bril: a novel bone-specific modulator of mineralization. *J Bone Miner Res* **23**, 1497–1508.

Mudhasani, R., Tran, J. P., Retterer, C., Radoshitzky, S. R., Kota, K. P., Altamura, L. A., Smith, J. M., Packard, B. Z., Kuhn, J. H. & other authors (2013). IFITM-2 and IFITM-3 but not IFITM-1 restrict Rift Valley fever virus. *J Virol* **87**, 8451–8464.

Omatsu, T., Bak, E. J., Ishii, Y., Kyuwa, S., Tohya, Y., Akashi, H. & Yoshikawa, Y. (2008). Induction and sequencing of Rousette bat interferon α and β genes. *Vet Immunol Immunopathol* **124**, 169–176.

Papenfuss, A. T., Baker, M. L., Feng, Z. P., Tachedjian, M., Crameri, G., Cowled, C., Ng, J., Janardhana, V., Field, H. E. & Wang, L. F. (2012). The immune gene repertoire of an important viral reservoir, the Australian black flying fox. *BMC Genomics* **13**, 261.

Perreira, J. M., Chin, C. R., Feeley, E. M. & Brass, A. L. (2013). IFITMs restrict the replication of multiple pathogenic viruses. *J Mol Biol* **425**, 4937–4955.

Provost, C., Jia, J. J., Music, N., Lévesque, C., Lebel, M. E., del Castillo, J. R., Jacques, M. & Gagnon, C. A. (2012). Identification of a new cell line permissive to porcine reproductive and respiratory syndrome virus infection and replication which is phenotypically distinct from MARC-145 cell line. *Virol J* **9**, 267.

Quan, P. L., Firth, C., Conte, J. M., Williams, S. H., Zambrana-Torrelio, C. M., Anthony, S. J., Ellison, J. A., Gilbert, A. T., Kuzmin, I. V. & other authors (2013). Bats are a major natural reservoir for hepaciviruses and pegiviruses. *Proc Natl Acad Sci U S A* **110**, 8194–8199.

Seim, I., Fang, X., Xiong, Z., Lobanov, A. V., Huang, Z., Ma, S., Feng, Y., Turanov, A. A., Zhu, Y. & other authors (2013). Genome analysis reveals insights into physiology and longevity of the Brandt's bat *Myotis brandtii*. *Nat Commun* **4**, 2212.

Shan, Z., Han, Q., Nie, J., Cao, X., Chen, Z., Yin, S., Gao, Y., Lin, F., Zhou, X. & other authors (2013). Negative regulation of interferon-induced transmembrane protein 3 by SET7-mediated lysine mono-methylation. *J Biol Chem* **288**, 35093–35103.

Siegrist, F., Ebeling, M. & Certa, U. (2011). The small interferon-induced transmembrane genes and proteins. *J Interferon Cytokine Res* **31**, 183–197.

Smith, I. & Wang, L. F. (2013). Bats and their virome: an important source of emerging viruses capable of infecting humans. *Curr Opin Virol* **3**, 84–91.

Smith, S. E., Gibson, M. S., Wash, R. S., Ferrara, F., Wright, E., Temperton, N., Kellam, P. & Fife, M. (2013). Chicken interferon-inducible transmembrane protein 3 restricts influenza viruses and lyssaviruses in vitro. *J Virol* **87**, 12957–12966.

Smith, S., Weston, S., Kellam, P. & Marsh, M. (2014). IFITM proteins-cellular inhibitors of viral entry. *Curr Opin Virol* **4**, 71–77.

Takahashi, S., Doss, C., Levy, S. & Levy, R. (1990). TAPA-1, the target of an antiproliferative antibody, is associated on the cell surface with the Leu-13 antigen. *J Immunol* **145**, 2207–2213.

Tong, S., Zhu, X., Li, Y., Shi, M., Zhang, J., Bourgeois, M., Yang, H., Chen, X., Recuenco, S. & other authors (2013). New World bats harbor diverse influenza A viruses. *PLoS Pathog* **9**, e1003657.

Wang, Z., Zhang, A., Wan, Y., Liu, X., Qiu, C., Xi, X., Ren, Y., Wang, J., Dong, Y. & other authors (2014). Early hypercytokinemia is associated with interferon-induced transmembrane protein-3 dysfunction and predictive of fatal H7N9 infection. *Proc Natl Acad Sci U S A* **111**, 769–774.

Warren, C. J., Griffin, L. M., Little, A. S., Huang, I. C., Farzan, M. & Pyeon, D. (2014). The antiviral restriction factors IFITM1, 2 and 3 do not inhibit infection of human papillomavirus, cytomegalovirus and adenovirus. *PLoS ONE* **9**, e96579.

Weidner, J. M., Jiang, D., Pan, X. B., Chang, J., Block, T. M. & Guo, J. T. (2010). Interferon-induced cell membrane proteins, IFITM3 and tetherin, inhibit vesicular stomatitis virus infection via distinct mechanisms. *J Virol* **84**, 12646–12657.

Wright, E., Temperton, N. J., Marston, D. A., McElhinney, L. M., Fooks, A. R. & Weiss, R. A. (2008). Investigating antibody neutralization of lyssaviruses using lentiviral pseudotypes: a cross-species comparison. *J Gen Virol* **89**, 2204–2213.

Yount, J. S., Moltedo, B., Yang, Y. Y., Charron, G., Moran, T. M., López, C. B. & Hang, H. C. (2010). Palmitoylome profiling reveals *S*-palmitoylation-dependent antiviral activity of IFITM3. *Nat Chem Biol* **6**, 610–614.

Yount, J. S., Karssemeijer, R. A. & Hang, H. C. (2012). *S*-Palmitoylation and ubiquitination differentially regulate interferon-induced transmembrane protein 3 (IFITM3)-mediated resistance to influenza virus. *J Biol Chem* **287**, 19631–19641.

Zhang, Z., Liu, J., Li, M., Yang, H. & Zhang, C. (2012). Evolutionary dynamics of the interferon-induced transmembrane gene family in vertebrates. *PLoS ONE* **7**, e49265.

Zhang, G., Cowled, C., Shi, Z., Huang, Z., Bishop-Lilly, K. A., Fang, X., Wynne, J. W., Xiong, Z., Baker, M. L. & other authors (2013a). Comparative analysis of bat genomes provides insight into the evolution of flight and immunity. *Science* **339**, 456–460.

Zhang, Y. H., Zhao, Y., Li, N., Peng, Y. C., Giannoulatou, E., Jin, R. H., Yan, H. P., Wu, H., Liu, J. H. & other authors (2013b). Interferon-induced transmembrane protein-3 genetic variant rs12252-C is associated with severe influenza in Chinese individuals. *Nat Commun* **4**, 1418.

Zhao, X., Guo, F., Liu, F., Cuconati, A., Chang, J., Block, T. M. & Guo, J. T. (2014). Interferon induction of IFITM proteins promotes infection by human coronavirus OC43. *Proc Natl Acad Sci U S A* **111**, 6756–6761.

Zhou, P., Cowled, C., Todd, S., Crameri, G., Virtue, E. R., Marsh, G. A., Klein, R., Shi, Z., Wang, L. F. & Baker, M. L. (2011). Type III IFNs in pteropid bats: differential expression patterns provide evidence for distinct roles in antiviral immunity. *J Immunol* **186**, 3138–3147.

Zhou, P., Cowled, C., Wang, L. F. & Baker, M. L. (2013). Bat Mx1 and Oas1, but not Pkr are highly induced by bat interferon and viral infection. *Dev Comp Immunol* **40**, 240–247.

Zufferey, R., Nagy, D., Mandel, R. J., Naldini, L. & Trono, D. (1997). Multiply attenuated lentiviral vector achieves efficient gene delivery in vivo. *Nat Biotechnol* **15**, 871–875.